Available online at www.sciencedirect.com
ScienceDirect
Spectrochimica Acta Part A 66 (2007) 118–125
SPECTROCHIMICA ACTA PART A
www.elsevier.com/locate/saa

# Conformation effects on the fluorescence spectra of europium and terbium complexes with a family of ether-amide type multipodal ligands

Ke-Wei Lei, Wei-Sheng Liu *, Min-Yu Tan

*Department of Chemistry and State Key Laboratory of Applied Organic Chemistry, College of Chemistry and Chemical Engineering, Lanzhou University, Lanzhou 730000, China*

Received 21 September 2005; received in revised form 2 December 2005; accepted 7 January 2006

**Abstract**

Three multipodal ligands: 3,3,7,7-tetra[*N*-methyl-*N*-phenyl(acetamide)-2-oxymethyl]-5-oxanonane ($L^a$), 3,3,7,7-tetra[*N*-ethyl-*N*-phenyl (acetamide)-2-oxymethyl]-5-oxanonane ($L^b$), 3,3,7,7-tetra[*N*-benzyl-*N*-phenyl(acetamide)-2-oxymethyl]-5-oxanonane ($L^c$) and their europium and terbium nitrate and perchlorate complexes were synthesized. The 12 complexes were characterized by elemental analysis, IR, fluorescence spectroscopy and conductivity. The novel cup-like crystal structure of the Eu(III) complex with $L^b$ and fluorescence emission properties of the complexes have also been studied. It has been showed that the nature of the anion has a great effect upon the composition of the complexes. The difference in the composition of the complexes results in the difference in the emission properties of them. The $[Ln(NO_3)_5]$ group is negatively effective to the fluorescence intensity of the nitrate complexes. The luminescence intensity of Ln(III) perchlorate complex is stronger than that of nitrate complex.
© 2006 Elsevier B.V. All rights reserved.

*Keywords:* Ether-amide type multipodal ligand; Lanthanide; Fluorescence; Nitrate; Perchlorate; Anion effect

## 1. Introduction

The development of luminescent probes and sensors [1] is the subject of intensive research both in natural and medical science [2,3]. Probes based on europium and terbium ions are of special interest because of the particularly suitable spectroscopic properties of these ions [2,4]. The main advantages of lanthanide chelates in fluorescence spectrometry are their large stokes shifts, narrow emission profiles and long fluorescence lifetimes [5,6]. These have led to use lanthanides as fluorescent probes for highly sensitive time-resolved fluorimetric immunoassays, metal ion coordination in proteins and structural studies of biological macromolecule [7]. And these properties have also been used to improve the sensitivity for lanthanide estimation by conventional spectrofluorimetry and laser induced spectrofluorimetry [8].

Amide-based crown ethers offer many advantages in extraction and analysis of the rare earth ions [9,10] because of their ring-like coordination structure and terminal group effects. The open-chain crown ethers containing amide groups possess suitable molecular structure: a chain with inflexible terminal groups. Therefore, they are excellent reagents for activating ion-selective electrodes and extracts of rare earth ions [11]. However, luminescent properties on open-chain crown ethers with lanthanide complexes have been rarely reported [12]. So we have designed a series of multi-functional ligands having both selective ability to enhance luminescence of lanthanide complexes by providing some of proper conjugate absorption groups suitable for energy transfer, i.e. the coordinating groups with cavities for lanthanide ions and amide-based crown ethers. With several suitably designed arms, the multipodal ligands could shield the encapsulated lanthanide ions from interaction with the surroundings, and by deliberate incorporation of appropriate multiple absorption groups suitable for energy transfer, they could be used to develop strong luminescent lanthanide complexes.

* Corresponding author. Tel.: +86 931 8912552; fax: +86 931 8912582.
*E-mail address:* liuws@lzu.edu.cn (W.-S. Liu).

1386-1425/$ – see front matter © 2006 Elsevier B.V. All rights reserved.
doi:10.1016/j.saa.2006.01.053

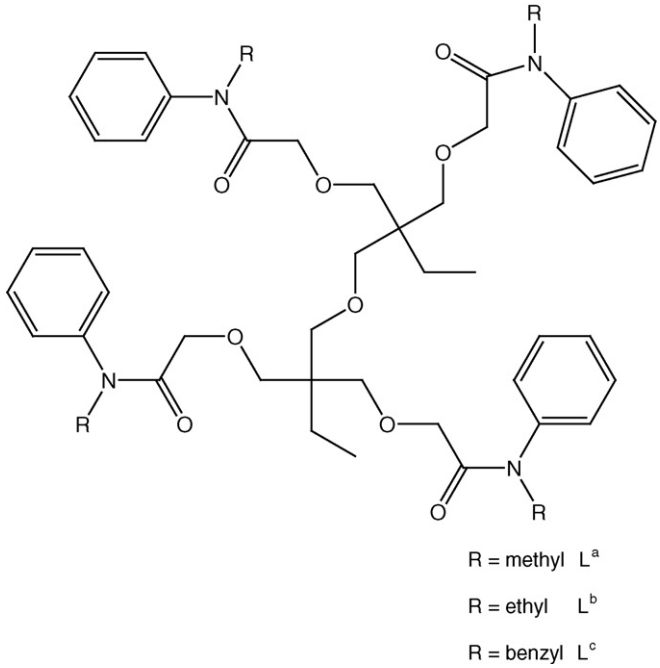


Scheme 1. The ligands.

In the recent work, we designed and synthesized a family of open-chain crown ether ligands, 3,3,7,7-tetra[*N*-methyl-*N*-phenyl(acetamide)-2-oxymethyl]-5-oxanonane ($L^a$), 3,3,7,7-tetra[*N*-ethyl-*N*-phenyl(acetamide)-2-oxymethyl]-5-oxanonane ($L^b$), 3,3,7,7-tetra[*N*-benzyl-*N*-phenyl(acetamide)-2-oxymethyl]-5-oxanonane ($L^c$) (Scheme 1) and 12 europium and terbium nitrate and perchlorate complexes. The conformation effects on fluorescence properties of the complexes were investigated.

## 2. Experimental

### 2.1. Materials

All commercially available chemicals were of A.R. grade and all solvents used were purified by standard methods.

### 2.2. Methods

The metal ions were determined by EDTA titration using xylenal orange as indicator. C, H and N were determined using an Elementar Vario EL. Conductivity measurements were carried out with a DDS-307 type conductivity bridge using $10^{-3}$ mol dm$^{-3}$ solutions in acetone at 25 °C. IR spectra were recorded on Nicolet FT-170SX instrument using KBr discs in the 400–4000 cm$^{-1}$ region, $^1$H NMR spectra were measured on a Varian Mercury plus 300 M spectrometer in CDCl3 solution with TMS as internal standard. Fluorescence measurements were made on a Hitachi F-4500 spectrophotometer equipped with quartz curettes of 1 cm path length at room temperature. The excitation and emission slit widths were 2.5 nm.

Table 1
Crystal data and structure refinement for the single crystal of $[EuL^b]\cdot[Eu(NO_3)_5]\cdot(NO_3)$

| | |
|---|---|
| CCDC | 285256 |
| Formula | $C_{52}H_{70}Eu_2N_{10}O_{27}$ |
| $M_r$ | 1571.10 |
| Color | Colorless |
| $T$ (K) | 298(2) |
| Wavelength (Å) | 0.71073 |
| Crystal system | Monoclinic |
| Space group | $C_2/c$ |
| $a$ (Å) | 40.376(6) |
| $b$ (Å) | 21.911(3) |
| $c$ (Å) | 22.290(3) |
| $\beta$ (°) | 92.660(5) |
| $V$ (Å$^3$) | 19698(5) |
| $Z$ | 12 |
| $D_x$/Mg (m$^3$) | 1.589 |
| $\theta$ (°) | 25.03 |
| $F$(0 0 0) | 9528 |
| Crystal size (mm) | 0.19 × 0.17 × 0.11 |
| $\theta$ Range (°) | 1.78–25.03 |
| Reflections collected | 50961 |
| Independent reflections | 17244 |
| Absorption correction | Multi-scab |
| Maximum and minimum transmission | 0.8116 and 0.7047 |
| Refinement method | Full-matrix least-squares on $F^2$ |
| Goodness-of-fit on $F^2$ | 0.968 |
| Final $R$ indices [$I > 2\sigma(I)$] | $R_1 = 0.0814$, $wR_2 = 0.1884$ |
| Largest diff. peak and hole (eÅ$^{-3}$) | 0.993 and −1.131 |

$w = 1/[s^2(Fo^2) + (0.0510P)^2 + 0.0000P]$; $P = (Fo^2 + 2Fc^2)/3$.

Table 2
Selected bond lengths (Å) and angles (°) for crystal of $[EuL^b]\cdot[Eu(NO_3)_5]\cdot(NO_3)$

| | | | |
|---|---|---|---|
| Eu(1)–O(9) | 2.339(9) | Eu(1)–O(3) | 2.351(9) |
| Eu(1)–O(5) | 2.394(9) | Eu(1)–O(7) | 2.396(9) |
| Eu(1)–O(2) | 2.424(9) | Eu(1)–O(8) | 2.442(9) |
| Eu(1)–O(1) | 2.448(8) | Eu(1)–O(4) | 2.533(9) |
| Eu(1)–O(6) | 2.543(9) | Eu(1)–C(44) | 3.195(16) |
| Eu(1)–C(8) | 3.225(15) | Eu(1)–C(34) | 3.254(17) |
| O(9)–Eu(1)–O(3) | 82.5(3) | O(9)–Eu(1)–O(5) | 70.8(3) |
| O(3)–Eu(1)–O(5) | 74.8(3) | O(9)–Eu(1)–O(7) | 72.8(3) |
| O(3)–Eu(1)–O(7) | 71.4(3) | O(5)–Eu(1)–O(7) | 132.6(3) |
| O(9)–Eu(1)–O(2) | 138.9(3) | O(3)–Eu(1)–O(2) | 64.3(3) |
| O(5)–Eu(1)–O(2) | 118.5(3) | O(7)–Eu(1)–O(2) | 74.1(3) |
| O(9)–Eu(1)–O(8) | 63.9(3) | O(3)–Eu(1)–O(8) | 139.0(3) |
| O(5)–Eu(1)–O(8) | 72.4(3) | O(7)–Eu(1)–O(8) | 116.0(3) |
| O(2)–Eu(1)–O(8) | 155.6(3) | O(9)–Eu(1)–O(1) | 138.5(3) |
| O(3)–Eu(1)–O(1) | 139.0(3) | O(5)–Eu(1)–O(1) | 112.5(3) |
| O(7)–Eu(1)–O(1) | 114.8(3) | O(2)–Eu(1)–O(1) | 78.2(3) |
| O(8)–Eu(1)–O(1) | 77.4(3) | O(9)–Eu(1)–O(4) | 132.7(3) |
| O(3)–Eu(1)–O(4) | 81.4(3) | O(5)–Eu(1)–O(4) | 62.1(3) |
| O(7)–Eu(1)–O(4) | 140.0(3) | O(2)–Eu(1)–O(4) | 67.8(3) |
| O(8)–Eu(1)–O(4) | 103.8(3) | O(1)–Eu(1)–O(4) | 69.1(3) |
| O(9)–Eu(1)–O(6) | 81.6(3) | O(3)–Eu(1)–O(6) | 133.2(3) |
| O(5)–Eu(1)–O(6) | 137.8(3) | O(7)–Eu(1)–O(6) | 61.9(3) |
| O(2)–Eu(1)–O(6) | 103.3(3) | O(8)–Eu(1)–O(6) | 66.9(3) |
| O(1)–Eu(1)–O(6) | 69.3(3) | O(4)–Eu(1)–O(6) | 138.4(3) |

Table 3
Analytical and molar conductance data for the complexes (calculated values in parentheses)

| Complexes | C | H | N | Ln | $\Lambda m$ (s cm$^2$ mol$^{-1}$) |
|---|---|---|---|---|---|
| [EuL$^a$]·[Eu(NO$_3$)$_5$]·(NO$_3$) | 38.14 (38.05) | 4.23 (4.12) | 9.16 (9.25) | 20.89 (20.06) | 180 |
| [TbL$^a$]·[Tb(NO$_3$)$_5$]·(NO$_3$) | 38.12 (37.71) | 4.12 (4.09) | 9.08 (9.16) | 20.65 (20.79) | 176 |
| [EuL$^b$]·[Eu(NO$_3$)$_5$]·(NO$_3$) | 39.85 (39.75) | 4.55 (4.49) | 8.85 (8.92) | 19.28 (19.35) | 193 |
| [TbL$^b$]·[Tb(NO$_3$)$_5$]·(NO$_3$) | 39.51 (39.40) | 4.37 (4.45) | 8.89 (8.84) | 19.98 (20.05) | 185 |
| [EuL$^c$]·[Eu(NO$_3$)$_5$]·(NO$_3$) | 48.01 (47.53) | 4.39 (4.32) | 7.85 (7.70) | 16.58 (16.71) | 167 |
| [TbL$^c$]·[Tb(NO$_3$)$_5$]·(NO$_3$) | 47.06 (47.17) | 4.20 (4.29) | 7.52 (7.64) | 17.69 (17.34) | 171 |
| [EuL$^a$]·(ClO$_4$)$_3$ | 44.85 (44.71) | 4.72 (4.83) | 4.24 (4.35) | 11.26 (11.79) | 321 |
| [TbL$^a$]·(ClO$_4$)$_3$ | 44.41 (44.47) | 4.80 (4.82) | 4.50 (4.32) | 12.31 (12.26) | 342 |
| [EuL$^b$]·(ClO$_4$)$_3$ | 46.48 (46.42) | 5.28 (5.24) | 4.20 (4.16) | 11.24 (11.29) | 332 |
| [TbL$^b$]·(ClO$_4$)$_3$ | 46.12 (46.18) | 5.28 (5.22) | 4.18 (4.14) | 11.85 (11.75) | 348 |
| [EuL$^c$]·(ClO$_4$)$_3$ | 54.19 (54.26) | 4.89 (4.93) | 3.57 (3.52) | 9.57 (9.54) | 336 |
| [TbL$^c$]·(ClO$_4$)$_3$ | 54.12 (54.02) | 4.22 (4.91) | 3.54 (3.50) | 9.87 (9.93) | 327 |

### 2.3. Synthesis of the ligand

A solution of 3,3,7,7-tetrahydroxymethyl-5-oxanonane (2.5 g, 10 mmol) in THF was added dropwise into a THF solution that was suspended with NaH (1.6 g, 60%, 40 mmol), and the mixture was stirred under nitrogen at room temperature until no gas appeared. Then a solution of *N*-ethyl-*N*-phenylchloroacetamide (8.7 g, 44 mmol) (*N*-methyl-*N*-phenylchloroacetamide for L$^a$, *N*-benzyl-*N*-phenylchloroacetamide for L$^c$) in THF was added dropwise into the mixture. After the mixture was refluxed for 6 h, the THF was evaporated and the residue was washed by column chromatography (silica gel, 2:1 CHCl$_3$/CH$_3$CO$_2$Et) and evaporated in vacuum resulted a yellow oil (4.3 g), yield: 50%. L$^a$, $^1$H NMR spectrum (300 M, CDCl$_3$): $\delta$ = 7.13–7.38 (m, 20 H); 3.73 (s, 8H; 4O–CH$_2$–C(O)); 3.22 (s, 12H; 4N–CH$_3$); 3.21 (s, 8H; 4C–CH$_2$–O); 2.98 (s, 4H; 2C–CH$_2$–O); 1.23 (q, 4H; 2R–CH$_2$–C); 0.70 (t, 6H; 2CH$_3$–R–C). IR: $\nu$ 1674s (C=O), 1112s (Ar–O–C). Formula weight of L$^a$: 839.45. Analytical data (%), C 68.67 (calc. 68.71); H 7.39 (7.45); N 6.56 (6.68).

L$^b$, $^1$H NMR spectrum (300M, CDCl$_3$): $\delta$ = 7.06–7.36 (m, 20H); 3.66 (s, 8H; 4O–CH$_2$–C(O)); 3.65 (q, 8H; 4N–CH$_2$–R); 3.17 (s, 8H; 4C–CH$_2$–O); 3.02 (s, 4H; 2C–CH$_2$–O); 1.21 (q, 4H; 2R–CH$_2$–C); 1.04 (t, 12H; 4CH$_3$–R–N); 0.70 (t, 6H; 2CH$_3$–R–C). IR: $\nu$ 1674s (C=O), 1122s (Ar–O–C). Formula weight of L$^b$: 895.13. Analytical data (%), C 69.77 (calc. 69.53); H 7.88 (7.97); N 6.26 (6.42).

L$^c$, $^1$H NMR spectrum (300M, CDCl$_3$): $\delta$ = 6.92–7.26 (m, 40H); 4.84 (s, 8H; 4N–CH$_2$–R); 3.75 (s, 8H; 4O–CH$_2$–C(O)); 3.23 (s, 8H; 4C–CH$_2$–O); 3.11 (s, 4H; 2C–CH$_2$–O); 1.27 (q, 4H; 2R–CH$_2$–C); 0.76 (t, 6H; 2CH$_3$–R–C). IR: $\nu$ 1675s (C=O), 1108s (Ar–O–C). Formula weight of L$^c$: 1142.58. Analytical data (%), C 75.77 (calc. 75.63); H 7.02 (6.88); N 5.06 (4.90).

### 2.4. Synthesis of complexes

An ethyl acetate solution of Ln(NO$_3$)$_3$·6H$_2$O [Ln = Eu(III), Tb(III), 0.2 mmol], Ln(ClO$_4$)$_3$·6H$_2$O [Ln = Eu(III), Tb(III), 0.1 mmol], was added dropwise to a solution of the ligand L (0.1 mmol) in the ethyl acetate (30 ml). The mixture was stirred for 4 h and white precipitate formed. The precipitate was collected and washed three times with ethyl acetate. Further drying in vacuum afforded pale white powder, yield: 75–80%.

Table 4
IR spectral data of the free ligands and their complexes (cm$^{-1}$)

| Compound | $\nu$(C=O) | $\nu$(C–O–C) | $\nu_1$(NO$_3^-$) | $\nu_3$(NO$_3^-$) | $\nu_4$(NO$_3^-$) | $\nu$(free) | $\nu_3$(ClO$_4^-$) | $\nu_4$(ClO$_4^-$) |
|---|---|---|---|---|---|---|---|---|
| L$^a$ | 1675 | 1112 | | | | | | |
| [EuL$^a$]·[Eu(NO$_3$)$_5$]·(NO$_3$) | 1623 | 1090 | 1490 | 816 | 1309 | 1384 | | |
| [TbL$^a$]·[Tb(NO$_3$)$_5$]·(NO$_3$) | 1624 | 1091 | 1492 | 816 | 1310 | 1384 | | |
| [EuL$^a$]·(ClO$_4$)$_3$ | 1623 | 1096 | | | | | 1097 | 942 |
| [TbL$^a$]·(ClO$_4$)$_3$ | 1624 | 1097 | | | | | 1098 | 946 |
| L$^b$ | 1675 | 1122 | | | | | | |
| [EuL$^b$]·[Eu(NO$_3$)$_5$]·(NO$_3$) | 1618 | 1095 | 1488 | 813 | 1308 | 1384 | | |
| [TbL$^b$]·[Tb(NO$_3$)$_5$]·(NO$_3$) | 1920 | 1095 | 1493 | 815 | 1310 | 1384 | | |
| [EuL$^b$]·(ClO$_4$)$_3$ | 1618 | 1098 | | | | | 1099 | 962 |
| [TbL$^b$]·(ClO$_4$)$_3$ | 1619 | 1099 | | | | | 1100 | 962 |
| L$^c$ | 1676 | 1108 | | | | | | |
| [EuL$^c$]·[Eu(NO$_3$)$_5$]·(NO$_3$) | 1616 | 1093 | 1492 | 816 | 1310 | 1384 | | |
| [TbL$^c$]·[Tb(NO$_3$)$_5$]·(NO$_3$) | 1621 | 1076 | 1495 | 826 | 1306 | 1384 | | |
| [EuL$^c$]·(ClO$_4$)$_3$ | 1619 | 1094 | | | | | 1095 | 926 |
| [TbL$^c$]·(ClO$_4$)$_3$ | 1620 | 1096 | | | | | 1098 | 922 |

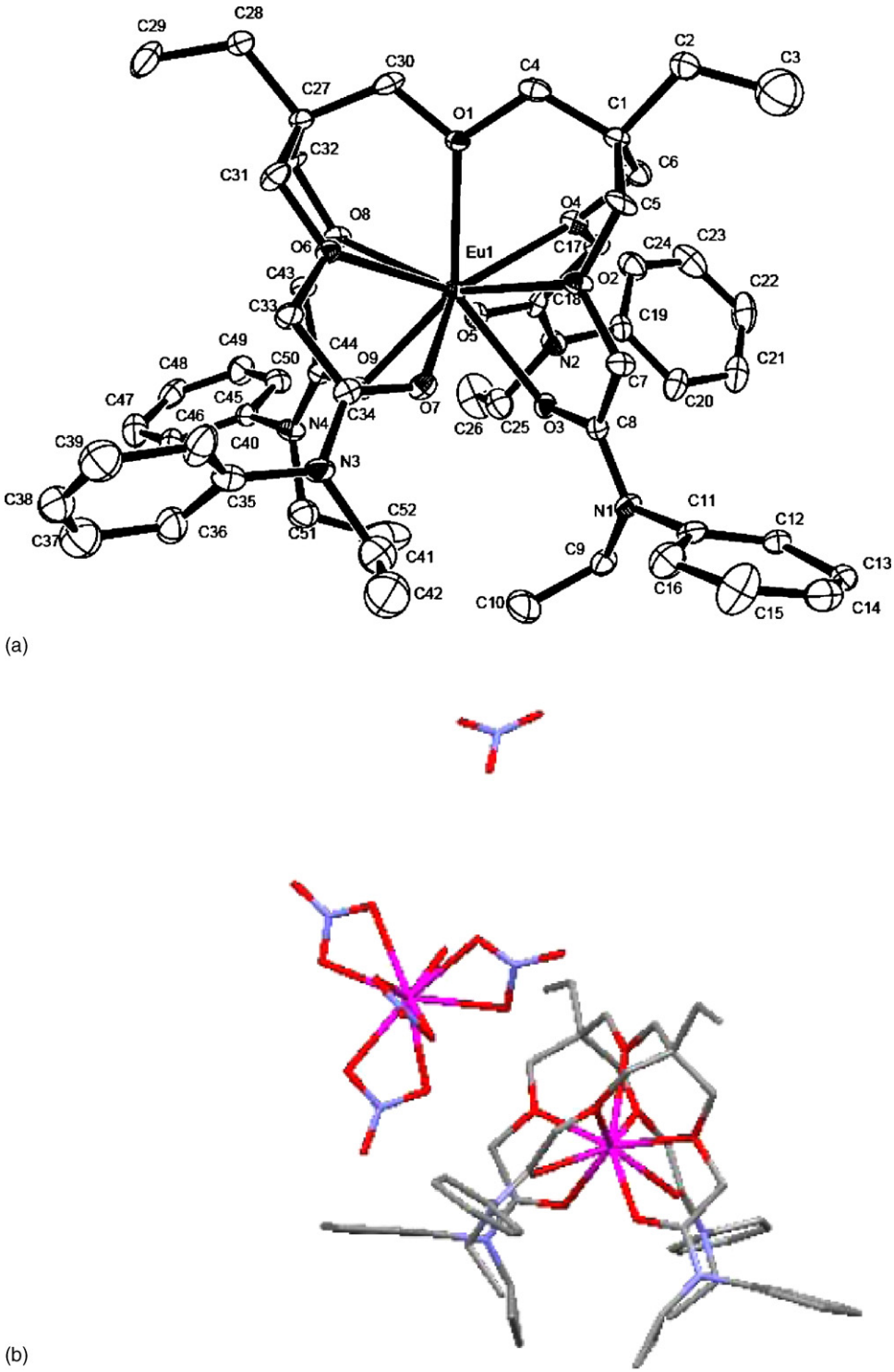


Fig. 1. (a) ORTEP diagram (30% probability ellipsoids) showing the coordination sphere of $[EuL^b]\cdot[Eu(NO_3)_5]\cdot NO_3$ with atom labeling scheme, H atoms attached to C atoms and $NO_3^{-1}$, $[Eu(NO_3)_5]^{-1}$ have been omitted for clarity; (b) molecular structure of $[EuL^b]\cdot[Eu(NO_3)_5]\cdot NO_3$.

### 2.5. X-ray crystallography

X-ray diffraction data were collected at 298(2) K on a CCD area detector diffractometer with graphite-monochromatized Mo Kα radiation (λ = 0.71073 Å). A summary of crystallographic data and details of the structure refinements are listed in Table 1. The structure was solved by direct methods and refined by full matrix least-squares techniques on $F^2$ with all non-hydrogen atoms treated anisotropically. All calculations were performed with the program package SHELXTL. The hydrogen atoms were assigned with common isotropic displacement factors and included in the final refinement by using geometrical

restrains. Selected bond lengths and angles are listed in Table 2.

## 3. Results and discussion

### 3.1. Properties of the complexes

Analytical data for the complexes listed in Table 3 conform to an 2:6:1 metal-to-nitrate-to-L stoichiometry $[LnL]\cdot[Ln(NO_3)_5]\cdot(NO_3)$, 1:3:1 metal-to-perchlorate-to-L stoichiometry $[LnL]\cdot(ClO_4)_3$. All complexes are soluble in DMF, acetonitrile, THF, MeOH, acetone, dioxane and CHCl3, but sparingly soluble in water and ethyl acetate. The molar conductances of the complexes in MeOH (see Table 3) indicate that all nitrate complexes act as 1:2 electrolytes, and all perchlorate complexes act as 1:3 electrolytes [13].

### 3.2. IR spectra

The main infrared bands of the ligand and its complexes are presented in Table 4. The IR spectrum of free ligand shows bands at 1674–1675 and 1122–1108 $cm^{-1}$, which may be assigned to $\nu$ (C=O) and $\nu$ (C–O–C), respectively. In the IR spectra of all the lanthanide complexes, these bands shift by about 50 and 25 $cm^{-1}$ toward lower wavenumbers, thus indicating that the carbonyl and ethereal oxygen atoms take part in coordination to the metal ion.

The absorption bands assigned to the coordinated nitrates were observed at about 1493 $cm^{-1}$ ($\nu_1$), 1311 $cm^{-1}$ ($\nu_4$) and 816 $cm^{-1}$ ($\nu_3$) for the complexes, respectively, implying that coordinated nitrate groups in the complexes are bidentate ligands [14]. The absorption band of about 1384 $cm^{-1}$ suggests that there is free nitrate in the complexes, which is in agreement with the results of the conductivity experiments.

### 3.3. X-ray crystallography

Fig. 1 shows the structure and the atomic numbering schemes for $[EuL^b]\cdot[Eu(NO_3)_5]\cdot(NO_3)$. As we can see from Figs. 1 and 2, L acts as a nonadentate ligand, four chains of it stretch around and form a cup-like cavity to encapsulate the metal ion with O atoms which can be described as a tricapped trigonal prism geometry (Fig. 3). We can see that five nitrates chelate a Ln ion to form a big counter anion (−2), one nitrate lies outside of the coordination sphere.

The bond lengths in complex are within normal ranges. The average distance between the Eu(III) ion and the coordination O atom is 2.428 Å. The Eu–O(C=O) distance (mean 2.369 Å) are significantly shorter than the Eu–O(Ar–O–C) distance (mean 2.486 Å). The Eu–O(C=O) bond is stronger than the Eu–O(Ar–O–C) bond.

### 3.4. Fluorescence studies

Under identical experimental, the fluorescence characteristics of the solid complexes are listed in Table 5. The ligands have strong antenna effect. So its terbium and europium complexes have moderate fluorescence. The fluorescence characteristic emission wavelengths of the terbium and europium ions were observed (Fig. 4). As shown in Fig. 4, the emission spectra of the six Eu complexes at room temperature are similar to each other and show characteristic emission bands of Eu(III) ion at about 594 and 616 nm, assigned to $^5D_0 \rightarrow {}^7F_1$ and $^5D_0 \rightarrow {}^7F_2$. The $^5D_0 \rightarrow {}^7F_3$ emission peaks are too weak to be observed at about 645–660 nm range [2]. The emission at about 616 nm from $^5D_0 \rightarrow {}^7F_2$ electronic dipole transition is the strongest, suggesting low symmetry around the Eu(III) ion [15]. Therefore, the peak height at 619 nm is used to measure the fluorescence intensities of europium complexes. We also see characteristic emission bands of Tb(III) ion at about 492, 546 and 586 nm, assigned to $^5D_4 \rightarrow {}^7F_6$, $^5D_4 \rightarrow {}^7F_5$ and $^5D_4 \rightarrow {}^7F_4$. The peak height of the strongest emission at about

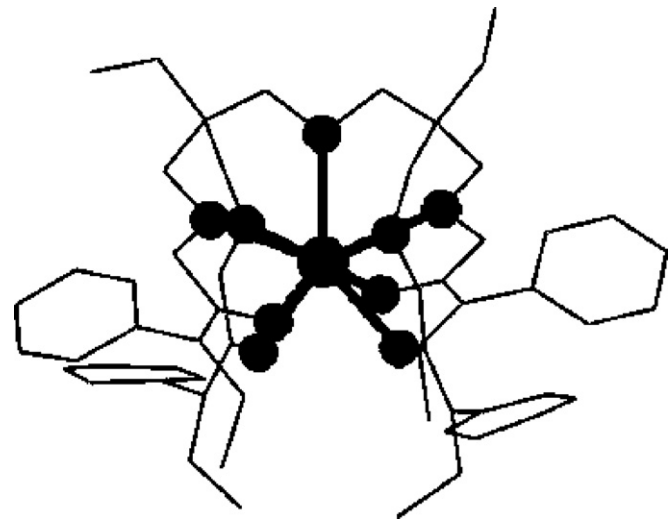

Fig. 2. Four chains of L stretch around Ln and form a cup-like cavity to encapsulate the metal ion.

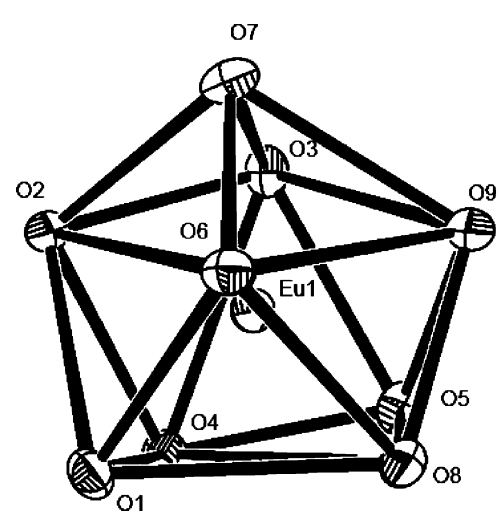


Fig. 3. The coordination polyhedron of the Eu(1) ion in $[EuL^b]\cdot[Eu(NO_3)_5]\cdot NO_3$.

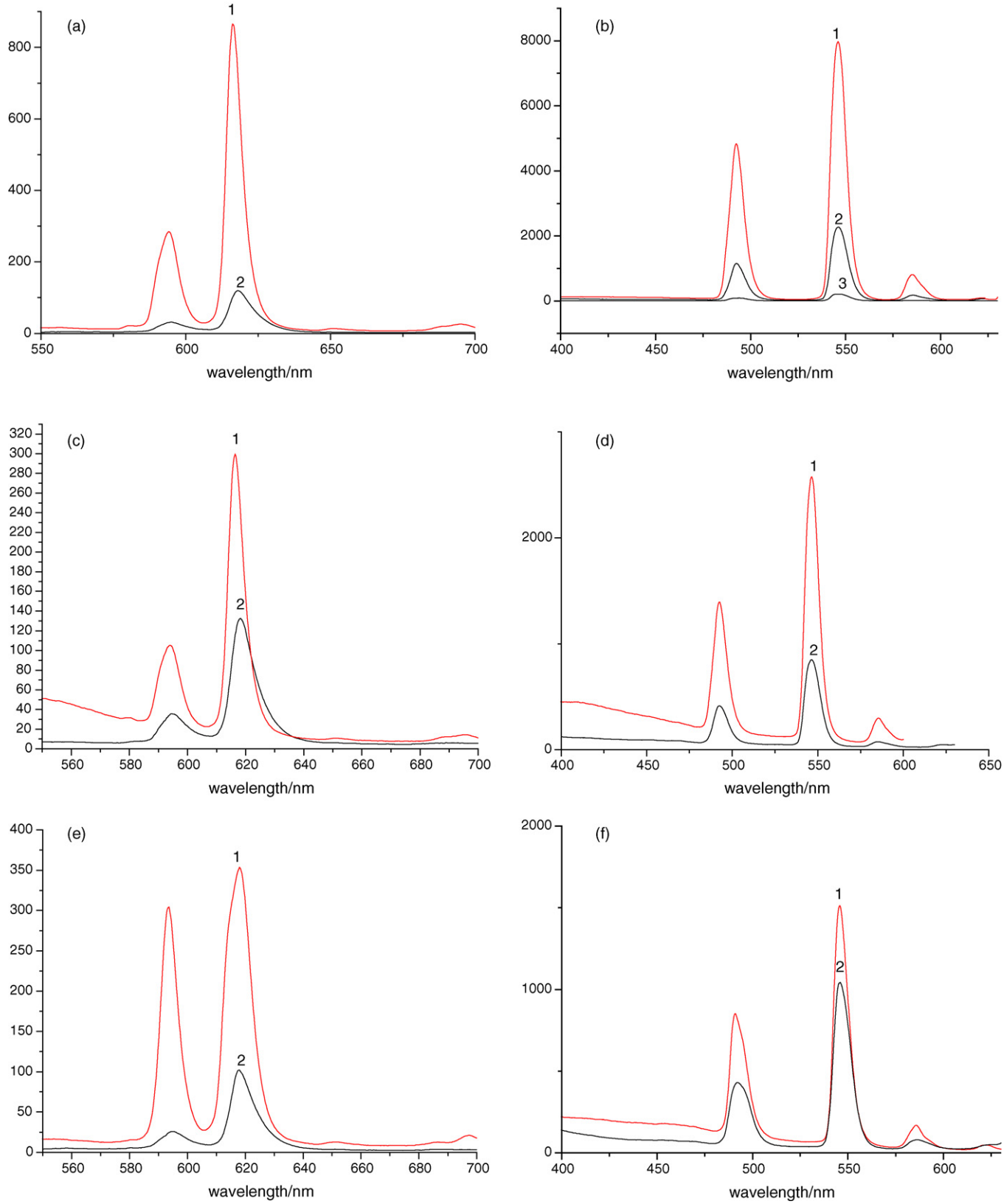


Fig. 4. (a) Emission spectra of the solid $[EuL^a]\cdot(ClO_4)_3$ (1) ($\lambda_{ex} = 398$ nm) and $[EuL^a]\cdot[Eu(NO_3)_5]\cdot(NO_3)$ (2) complex ($\lambda_{ex} = 399$ nm) at room temperature; (b) emission spectra of the solid $[TbL^a]\cdot(ClO_4)_3$ (1) ($\lambda_{ex} = 309$ nm), $[TbL^a]\cdot[Tb(NO_3)_5]\cdot(NO_3)$ (2) complex ($\lambda_{ex} = 319$ nm) and solid Tb nitrate (3) ($\lambda_{ex} = 320$ nm) at room temperature; (c) emission spectra of the solid $[EuL^b]\cdot(ClO_4)_3$ (1) ($\lambda_{ex} = 397$ nm) and $[EuL^b]\cdot[Eu(NO_3)_5]\cdot(NO_3)$ (2) complex ($\lambda_{ex} = 399$ nm) at room temperature; (d) emission spectra of the solid $[TbL^b]\cdot(ClO_4)_3$ (1) ($\lambda_{ex} = 306$ nm) and $[TbL^b]\cdot[Tb(NO_3)_5]\cdot(NO_3)$ (2) complex ($\lambda_{ex} = 321$ nm) at room temperature, (e) emission spectra of the solid $[EuL^c]\cdot(ClO_4)_3$ (1) ($\lambda_{ex} = 397$ nm) and $[EuL^c]\cdot[Eu(NO_3)_5]\cdot(NO_3)$ (2) complex ($\lambda_{ex} = 399$ nm) at room temperature, (f) emission spectra of the solid $[TbL^c]\cdot(ClO_4)_3$ (1) ($\lambda_{ex} = 354$ nm) and $[TbL^c]\cdot[Tb(NO_3)_5]\cdot(NO_3)$ (2) complex ($\lambda_{ex} = 320$ nm) at room temperature.

Table 5
Fluorescence data for the complexes

| Complexes | $\lambda_{ex}$ (nm) | $\lambda_{em}$ (nm) | RFI | Assignment |
|---|---|---|---|---|
| $[EuL^a]\cdot[Eu(NO_3)_5]\cdot(NO_3)$ | 399 | 595 | 34 | $^5D_0 \rightarrow {}^7F_1$ |
| | | 617 | 121 | $^5D_0 \rightarrow {}^7F_2$ |
| $[EuL^a]\cdot(ClO_4)_3$ | 398 | 594 | 285 | $^5D_0 \rightarrow {}^7F_1$ |
| | | 616 | 865 | $^5D_0 \rightarrow {}^7F_2$ |
| $[TbL^a]\cdot[Tb(NO_3)_5]\cdot(NO_3)$ | 319 | 493 | 1179 | $^5D_4 \rightarrow {}^7F_6$ |
| | | 546 | 2252 | $^5D_4 \rightarrow {}^7F_5$ |
| | | 586 | 189 | $^5D_4 \rightarrow {}^7F_4$ |
| $[TbL^a]\cdot(ClO_4)_3$ | 309 | 492 | 4807 | $^5D_4 \rightarrow {}^7F_6$ |
| | | 546 | 7998 | $^5D_4 \rightarrow {}^7F_5$ |
| | | 585 | 822 | $^5D_4 \rightarrow {}^7F_4$ |
| $[EuL^b]\cdot[Eu(NO_3)_5]\cdot(NO_3)$ | 399 | 595 | 35 | $^5D_0 \rightarrow {}^7F_1$ |
| | | 618 | 131 | $^5D_0 \rightarrow {}^7F_2$ |
| $[EuL^b]\cdot(ClO_4)_3$ | 397 | 594 | 105 | $^5D_0 \rightarrow {}^7F_1$ |
| | | 617 | 298 | $^5D_0 \rightarrow {}^7F_2$ |
| $[TbL^b]\cdot[Tb(NO_3)_5]\cdot(NO_3)$ | 321 | 492 | 413 | $^5D_4 \rightarrow {}^7F_6$ |
| | | 547 | 848 | $^5D_4 \rightarrow {}^7F_5$ |
| | | 586 | 82 | $^5D_4 \rightarrow {}^7F_4$ |
| $[TbL^b]\cdot(ClO_4)_3$ | 306 | 492 | 1385 | $^5D_4 \rightarrow {}^7F_6$ |
| | | 546 | 2574 | $^5D_4 \rightarrow {}^7F_5$ |
| | | 586 | 310 | $^5D_4 \rightarrow {}^7F_4$ |
| $[EuL^c]\cdot[Eu(NO_3)_5]\cdot(NO_3)$ | 399 | 595 | 26 | $^5D_0 \rightarrow {}^7F_1$ |
| | | 618 | 102 | $^5D_0 \rightarrow {}^7F_2$ |
| $[EuL^c]\cdot(ClO_4)_3$ | 397 | 593 | 302 | $^5D_0 \rightarrow {}^7F_1$ |
| | 320 | 618 | 352 | $^5D_0 \rightarrow {}^7F_2$ |
| $[TbL^c]\cdot[Tb(NO_3)_5]\cdot(NO_3)$ | | 491 | 854 | $^5D_4 \rightarrow {}^7F_6$ |
| | | 546 | 1506 | $^5D_4 \rightarrow {}^7F_5$ |
| | | 586 | 171 | $^5D_4 \rightarrow {}^7F_4$ |
| $[TbL^c]\cdot(ClO_4)_3$ | 354 | 492 | 433 | $^5D_4 \rightarrow {}^7F_6$ |
| | | 546 | 1041 | $^5D_4 \rightarrow {}^7F_5$ |
| | | 586 | 81 | $^5D_4 \rightarrow {}^7F_4$ |

RFI is relative fluorescence intensity.

546 nm from $^5D_4 \rightarrow {}^7F_5$ electronic dipole is used to measure the fluorescence intensities of Tb complexes. We can notice solid luminescence intensity of each Eu perchlorate complex is stronger than that of Eu nitrate complex with the same ligand, the case is the same with the Tb complexs (Fig. 4). This is due to the conformation effect [16]. It has been showed that the nature of the anion has a great effect upon the composition of the complexes. The difference in the composition of the complexes results in the difference in the emission properties of them. In the studied examples, the luminescence intensity of Ln(III) perchlorate complex is stronger than that of nitrate complex. We know that the complexes conform to $[LnL]\cdot[Ln(NO_3)_5]\cdot(NO_3)$ (nitrate complexes) and $[LnL]\cdot(ClO_4)_3$ (perchlorate complexes). In every complex, a ligand chelates a Ln ion with nine O atoms, but the counter-anions are different: $[Ln(NO_3)_5]^{2-}$ and $NO_3^-$ in nitrate complexes, $ClO_4^-$ in perchlorate complexes. Based on antenna effect [17,18], the intensity of the luminescence of $Ln^{3+}$ complexes is related to the efficiency of the intramolecular energy transfer between the triplet energy level of the ligand and the emitting level of the central ion, which depends on the gap between the two levels. As we know luminescence intensity of solid Ln (Ln = Eu, Tb) nitrate is poor (Fig. 4b), we consider that efficiency of energy transfer from $NO_3$ to Ln in $[Ln(NO_3)_5]$ is very poor, which results in incomplete energy transfer in the whole nitrate complex molecule though that from L to Ln is efficient. The $[Ln(NO_3)_5]$ group is negatively effective to the fluorescence intensity of the nitrate complexes.

## 4. Conclusion

According to the data and discussion above, the amide-based multipodal ligand could form complexes with lanthanide ions and exhibit a caverned conformation. The complexes exhibited characteristic fluorescence of europium and terbium ion, respectively. It has been showed that the nature of the anion has a great effect upon the composition of the complexes. The difference in the composition of the complexes results in the difference in the emission properties of them. The luminescence intensity of Ln(III) perchlorate complex is stronger than that of nitrate complex. Based on those results, a series of new amide-based multipodal derivatives could be designed and synthesized to optimize the luminescent properties of these lanthanide ions.

*Supplementary material*

Crystallographic data for the structure analysis have been deposited with the Cambridge Crystallographic Data Center, CCDC No. 285256. Copies of this information may be obtained free of charge from the Director, CCDC, 12 Union Road, Cambridge CB2 1EZ, UK (e-mails: linstead@ccdc.cam.ac.uk; deposit@ccdc.cam.ac.uk, direct line: +44 1223 762910; tel: +44 1223 336408; fax: +44 1223 336033).

## Acknowledgements

We are grateful to the NSFC (Grants 20371022, 20431010 and 20021001), the Specialized Research Fund for the Doctoral Program of Higher Education (200307300015), and the Key Project of the Ministry of Education of China (Grant 01170) for financial support.

## References

[1] N. Sabbatini, M. Guardigli, J.-M. Lehn, Coord. Chem. Rev. 123 (1993) 201.
[2] S.T. Frey, M.L. Gong, W. de Horrocks, Inorg. Chem. 33 (1994) 3229.
[3] N. Sato, S. Shinkai, J. Chem. Soc. Perkin Trans. 2 (1993) 621.
[4] C. Piguet, A.F. Williams, G. Bernardinelli, J.-C.G. Bünzli, Inorg. Chem. 32 (1993) 4139.
[5] F.S. Richardson, Chem. Rev. 82 (1982) 541.
[6] J.-C.G. Bünzli, in: J.-C.G. Bünzli, G.R. Choppin (Eds.), Lanthanide Probes in Life, Chemical and Earth Sciences, Elsevier, Amsterdam, 1989 (Chapter 7).
[7] B.S. Panigrahi, Spectrochim. Acta A 56 (2000) 1337.
[8] C. Piguet, J.-C.G. Bünzli, G. Bernardinelli, G. Hopfgartner, S. Petoud, O. Schaad, J. Am. Chem. Soc. 118 (1996) 6681.
[9] Y.-S. Yang, S.-H. Cai, Hua Xue Shi Ji 6 (1984) 133.
[10] Y.Z. Ding, J.Z. Lu, Y.S. Yang, Hua Xue Shi Ji 8 (1986) 201.

[11] G.Z. Tan, J.Z. Xu, T.Q. Jiao, You Ji Hua Xue 2 (1986) 143.
[12] W. Yang, X.L. Teng, M. Chem, Talanta 46 (1998) 527.
[13] W.J. Gear, Coor. Chem. Rev. 7 (1971) 81.
[14] K. Nakamoto, Infrared and Raman spectra of Inorganic and Coordination Compounds, 3rd ed., John Wiley, New York, 1978, p. 227.
[15] R.M. Silverstein, G.C. Bassler, T.C. Morrill, Spectrometric Identification of Organic Compound, 5th ed., Wiley, New York, 1991.
[16] John Coates, Elaine Gay, Peter G. Sammes, Dyes Pigments 34 (1997) 195.
[17] J.-M. Lehn, Angew. Chem. Int. Ed. Engl. 29 (1990) 1304.
[18] M. Latva, H. Takalo, K. Simberg, J. Kankare, J. Chem. Soc. Perkin Trans. 2 (1995) 995;
M. Latva, H. Takalo, K. Simberg, J. Kankare, Polyhedron 16 (1997) 1381.